Journal of Theoretical and Applied Physics (JTAP), Special Issue: AICIS'23-Article 03

Proceeding of the 3rd Annual International Conference on Information and Sciences 2023, University of Fallujah, Iraq

https://dx.doi.org/10.57647/j.jtap.2024.si-AICIS23.03

Investigate the structural, morphological, and topographical characteristics of CuO thin films utilizing a pulsed laser deposition method

Abeer Mohammed Enad, Jamal M. Rzaij*

Department of Physics, College of Science, University Of Anbar, Ramadi, Iraq.

***Corresponding author:** sc.jam72al@uoanbar.edu.iq

Original Research

Published online: 15 June 2024

Abstract:

In this work, copper oxide (CuO) thin films were prepared using the pulsed laser deposition (PLD) technique. The effect of laser beam energy and pulse number on the structural, morphological, and topographical characteristics was investigated. X-ray diffraction (XRD) results indicate the presence of characteristic peaks for CuO with a crystalline growth orientation at the (111) plane and an increase in crystallite size (D) when the laser power and number of pulses increase. EDX results indicate the presence of distinct energy peaks for the copper and oxygen elements that form CuO, and the weight percentage (wt.%) of Cu increases with increasing laser energy. The atomic force microscope (AFM) results showed the dependence of the roughness on the laser energy used, as the roughness decreased from 31.18 to 20.89 nm when the energy increased from 700 to 820 mJ. It increases with the increase in the number of laser pulses at the same energy (700 mJ). Field emission scanning electron microscopy (FESEM) confirms the presence of sub-spherical nanoparticles, and increasing laser energy and pulses increases nanoparticle size.

Keywords: PLD; Structural and morphological; CuO; Thin-films; Metal oxide; Characterization

1. Introduction

Thin films, seen as two-dimensional ($2D$) systems, hold significant importance in various fields and possess distinct features that vary from those exhibited by bulk materials [1]. Innovations in the fields of magnetic recording media, electronic semiconductor devices, gas sensing, light-emitting diodes, optical coatings, photo-detector, hard coatings on cutting tools, and energy generation and storage batteries were all made possible by developments in thin film deposition technique [2]. The chemical and physical properties of a material's bulk can be affected by its nanostructure, defined as having at least one dimension smaller than 100 nm [3]. As a result, there has been a rise in the fabrication of nanoscale structures worldwide, which are then used as the foundation for nanotechnology. The nanoparticles, nanobeams, nanowires, nanoribbons, nanotubes, nanoplates, and components of nanomachines are all examples of structures on the nanoscale [4]. Nanoparticles are particles with nanometer-scale dimensions ($1-100$ nm). It has better colloidal stability and optical, chemical, electrical, thermal, and mechanical properties than larger particles because of their small size and high surface area [5].

The term "metal oxide" (MO) refers to a group of minerals in which one or more metal ions have formed covalent bonds with oxygen ions (O^{2-}). Minerals that include hydroxides are also classified as oxides. The most widely used metal oxides include zinc oxide, titanium dioxide, iron oxide, nickel oxide, selenium oxide, silicon oxide, magnesium oxide, manganese oxide, and copper oxide [6]. Benefits of MOs include their simplicity in preparation, high stability, shape, and porosity, amenability to engineering to the desired size, lack of swelling variation, adaptability to both hydrophilic and hydrophobic systems, and fast sensing and detection of another chemical material [7].

In contrast, copper oxide is one of the most studied nanomaterials because it has a direct band gap of $1.2-2.0$ eV, an intrinsic p-type behavior, excellent electrochemical properties, and can be fabricated inexpensively. Cuprous oxide (Cu_2O) and CuO are the two most prevalent polymorphs

of CuO compounds [7]. CuO nanoparticles have been utilized in a wide range of applications, including magnetic storage media, nanosensors, near-infrared filters, photocatalysis, antibacterial agents, and supercapacitors [8]. In the same vein, various techniques have been employed to fabricate CuO nanoparticles, such as green synthesis, sol-gel method, laser ablation, microwave-assisted, and chemical precipitation methods [9]. Pulsed laser deposition (PLD) is commonly employed to enhance oxide films due to its advantageous ability to preserve stoichiometry in complex materials. However, a limited number of studies have investigated the growth of CuO using this technique. Nevertheless, it has been observed that the PLD of CuO can produce films with improved properties [10].

The Deposition of thin films can be accomplished through various physical and chemical techniques [11–15]; however, tpulsed laser deposition possesses features that distinguish it from the others. A. A. Menazea et al., prepared thin copper oxide films using the PLD technique. The optical, structural, and morphological properties were studied, but the effect of changing the laser parameters (laser power and number of pulses) on the film thickness was not studied [10]. Rudrashish et al. used the PLD technique to prepare thin films of Cu_2O/CuO and then studied their application inphotocatalysis. The authors succeeded in preparing thin films with a uniform shape. Still, the effect of preparing thin films of different thicknesses by increasing or decreasing the number of laser pulses or their energy has not been studied [16]. Majed H. Dwech et al. studied the effect of increasing the number of laser pulses on the thickness of the thin film of CuO prepared using the PLD technique. Only the optical properties were studied without investigating the increase in the number of pulses on the surface roughness, nanoparticle shape, and structure properties. Also, the effect of increasing the laser beam energy on the properties of the oxide has not been studied. This work aims to prepare CuO thin films by an inexpensive PLD method. The effect of increasing the number of pulses from 600 to 1000 pulses, and increasing the energy change from 700 to 820 mJ, on the structural, morphological, and topographical properties of the CuO thin film was studied.

2. Experimental work and characterization

A high-purity CuO powder, with a purity of 99.99%, is subjected to a pressing process utilizing a pressure of 15 tons. This process results in formaing a target with a diameter of 2 cm and a thickness of 0.5 cm. The PLD technique was employed to produce thin films of CuO on glass substrates at room temperature, resulting in a film thickness of around 100 nm. The film deposition process was conducted within a vacuum chamber that had been evacuated to a pressure of 2.2×10^{-2} millitorr. The chamber was equipped with substrate holders and a target. The substrate was positioned close to the target, with its surface oriented parallelly. To enhance the quality of films, it is imperative to make modifications to the deposition procedure, which include adjustments to both the target-substrate positioning and the target rotation. The separation between the substrate and the target is 2 cm, whereas the separation between the laser source and the target is 5 cm. The system operates at a temperature of 28 °C, a wavelength of 1064 nm, and a repetition frequency of 6 Hz.

At room temperature, a Dandong Haoyuan DX-2700B X-ray diffractometer with a Cu-K radiation source was used to study the structures of the crystals. A diffraction angle (2θ) range of 10° - 80° and X-ray wavelength of 1.54056 $\AA$. An atomic force microscope (AFM, NaioAFM, Nanosurf; Switzerland) was used to measure the roughness and average diameter of CuO thin films. The Field Emission Scanning Electron Microscope (FESEM; MIRA3 model-TE-SCAN) was used to determine the surface morphology of CuO thin films.

3. Results and discussion

3.1 X-ray diffraction (XRD) analysis

Fig. 1 shows the XRD spectra of CuO thin film deposited on glass substrates by PLD technique at (1000) pulses with energy of (700 and 820 mJ). The results indicate diffraction peaks of different intensities and widths at different diffraction angles. These peaks correspond to the planes (110), (-111), (111), (20-2), (020), (202), (-113), (31-1), (220), (311), and (22-2). which correspond to JCPDS card No. 96-101-1195 of the CuO monoclinic phase [16]. The dominant diffraction peaks at energy 700 and 820 mJ were at (111) and (-111). Increasing the energy of the pulsed laser contributes to an increase in the diffraction intensity of the incident X-rays due to the increase in the thickness of the thin film (number of nanoparticles bonded to each other due to surface bonding). This high crystallinity can be used in gas-sensing applications [17].

The results did not show the presence of any additional impurities in the prepared sample, thus enhancing the purity of the thin films. The present results agree with the results of references [18, 19]. Table 1 shows the XRD parameters of CuO thin film at (1000) pulses with energy of (700 and 820 mJ). Further investigation on crystallinity was conducted. The crystallite size (D) of the deposited CuO thin films was estimated using Scherrer's formula [20].

$$D = \frac{0.9 \times \lambda}{\beta \times \cos\theta} \tag{1}$$

where θ is the diffraction angle, λ is the wavelength of XRD spectra, and β is the full width at half maximum (FWHM) of the peaks. According to the data shown in Table 1, it can be concluded that the average crystal size across all planes was determined to be 14.854 nm at 700 mJ and 18.30 nm at 820 mJ. This increase in crystalline size as a result of the increase in energy can be attributed to the increase in temperature, plasma, and the size of the extracted particles, and thus the increase in the binding potential of small atoms with each other.

Fig. 2 shows the XRD pattern of CuO thin film that was prepared at (700) mJ with pulses of 600 and 1000. The results also confirm the presence of characteristic peaks corresponding to the planes (110), (-111), (111), (2-20), (020), (202), (-113), (13-1), (220), (311), and (22-2), which correspond to data of JCPDS card No. 96-101-1195 of the CuO monoclinic phase. As shown in Table 2, the results

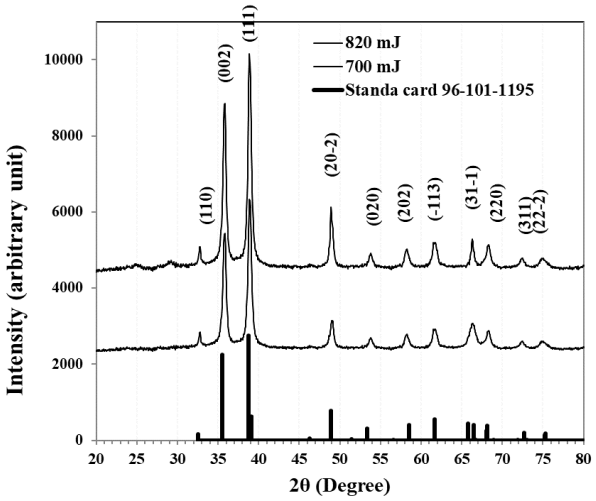

Figure 1. XRD patterns for CuO deposited at 1000 pulses and energies of 700 and 820 mJ.

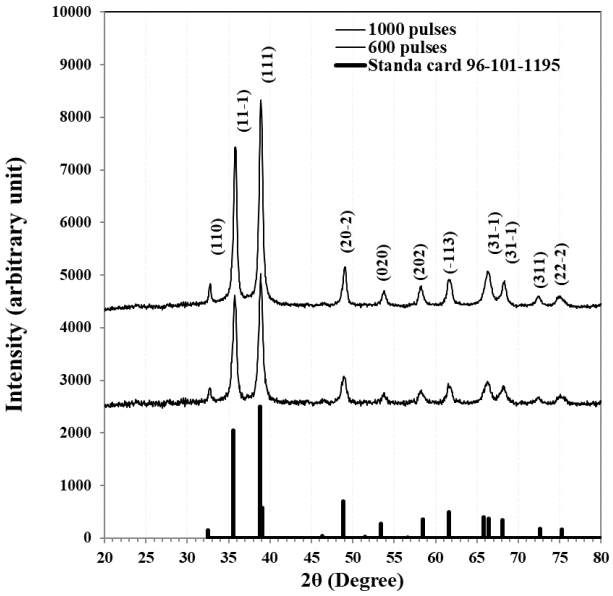

Figure 2. XRD patterns of CuO deposited with 700 mJ at 600 and 1000 pulses.

indicate an increase in crystal size from 10.21 nm at 600 pulses to 14.85 nm at 1000 pulses. This increase can be attributed to the increased concentrations of CuO ions. As a result of this increase, different surface forces (electrostatic ionic forces, Vander Waals forces, structural forces, and static forces) can contribute to the aggregation of ions with each other and, thus, an increase in crystal size [21].

3.2 EDX analysis results

The chemical composition of the CuO thin film was confirmed by EDX analysis, as shown in Fig. 3(a) and (b). The results show the presence of sharp energy peaks for the O and Cu elements representing the CuO nanostructure. The purity of the manufactured films was excellent, and they did not contain any residues (except Si, Ca, Mg, and Na elements that belong to the constituent elements of the glass substrate). The energy peak at 2.2 keV is attributed to the gold layer that the samples were coated with before testing. The present results support the XRD results and are largely in agreement with the results of reference [22].
Table 3 presents each condition's weight percentage (Wt.%) of the O and Cu elements. The results confirm a significant increase in the Wt.% of Cu in the thin film when the pulsed laser energy is increased from 700 to 820 mJ. This could be due to the increase in the energy of the laser photons that release ions from the surface of the metal target.

3.3 Topographical analysis

The films' surface topography and surface roughness were studied using the AFM technique. Fig. 4 displays AFM topography images of CuO thin films deposited on glass substrates prepared by the PLD technique. Table 4 displays the measured roughness characteristics for the CuO films, which correspond to varying laser pulse energies of 700 and 820 mJ and pulse counts of 1000 and 600. The film showed a homogeneous distribution, and the grain shapes were almost uniform. The results indicate an increase in surface roughness from 26.58 nm to 31.18 nm due to increasing the number of pulses from 600 to 1000. In the same context, the results showed the dependence of roughness on the laser energy used, as the roughness decreased from 31.18 nm to

Table 1. Structure parameters of CuO deposited at 1000 pulses and energies of 700 and 820 mJ.

Laser energy (mJ)	2θ (deg.)	FWHM (deg.)	d_{hkl} Exp.(Å)	D (nm)	d_{hkl} Std.(Å)	hkl
700	38.8897	0.5019	2.3139	16.8	2.3212	-111
820	38.874	0.429	2.3148	19.6	2.3212	-111

Table 2. The structure parameter of CuO deposited with 700 mJ at 600 and 1000 pulses.

Pulses	2θ (deg.)	FWHM (deg.)	d_{hkl} Exp.(Å)	D (nm)	d_{hkl} Std.(Å)	hkl
600	38.8441	0.7301	2.3165	11.5	2.3212	-111
1000	38.8897	0.5019	2.3139	16.8	2.3212	-111

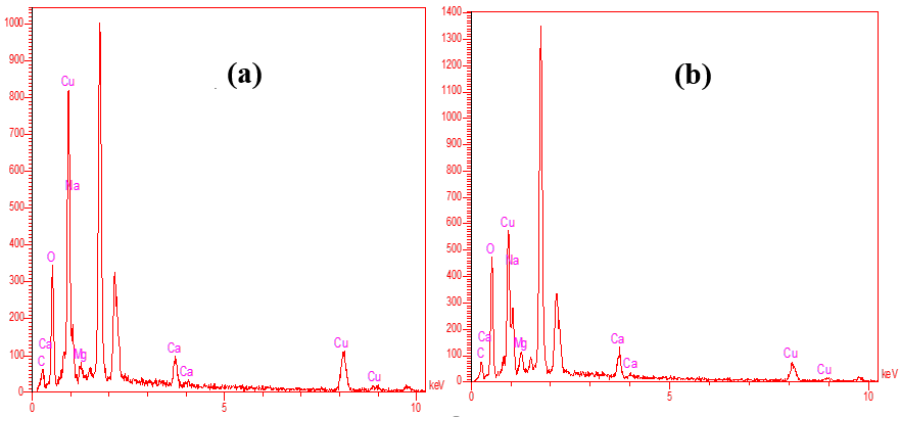

Figure 3. EDX spectra of CuO thin-film prepared at (a) 700 mJ/600 pulses and (b) 820 mJ/1000 pulses.

20.89 nm when the energy increased from 700 to 820 mJ. This behavior can be attributed to the small diameter of nanoparticles and the ideal interaction between micro/-nanoparticles (see histogram in Fig. 4), which can contribute to the enhancement and increase in roughness [23]. Based on the analysis of X-ray diffraction and topography of the deposited films, it is evident that there is a consistent trend of increasing average crystal size and grain size with increasing energy and pulse number of the laser ablation. However, it is worth noting that the sample prepared with 700 mJ and 1000 pulses exhibited a decrease in average diameter, deviating from this overall sequence. The observed decline in average diameter can be attributed to an increase in the number of border interfaces and boundaries of grains per unit area, resulting in a reduction in grain size [24, 25].

3.4 Microstructure results

The surface morphology and the histogram of atom distribution of CuO thin films are shown in Fig. 5. The top view of the film deposited at 700 mJ/600 pulses is revealed in Fig. 5(a); the results indicate the presence of a distribution of semi-spherical nanoparticles with an average particle size of about 16.56 nm (Fig. 5(d)). Fig. 5(b) revealed the top view of the film deposited at 700 mJ/1000 pulses, the results confirm the presence of small, spherical nanoparticles with an average particle size of about 12 nm (Fig. 5(e)).
Fig. 5(c) revealed the top view of the film deposited at 820 mJ/1000 pulses; the results showed the appearance of an agglomeration of nanoparticles with an average particle size of about 13 nm (Fig. 5(f)). Fig. 5(b-f) confirmed an increase in the distribution of nanoparticles with an increase in the number of laser pulses, and this can be attributed to the stability of the particles extracted from the target surface at the energy of 700 mJ. Moreover, increasing the laser energy to 820 mJ contributes to increasing the size due to the increased concentration of particles extracted from the target surface, and this leads to enhanced agglomeration of small particles due to the high reactivity of the free electrons in the outer shells [26, 27]. The FE-SEM results match the AFM results in nanoparticle size dependence on laser energy and pulses.

4. Conclusion

According to the results, it can be concluded that the PLD technique is effective in preparing CuO thin films. XRD results show sharp diffraction peaks attributed to highly crystalline CuO monoclinic without impurities. Scherer equation indicated an increase in the size of the crystals when the energy of the laser beam and its pulses increased. EDX results show that the highest weight of Cu metal was achieved when the laser energy was increased to 820 mJ. AFM results confirmed a decrease in roughness from 31.18 nm to 20.89 nm with increasing laser power from 700 to 820 mJ. The small diameter of nanoparticles and ideal micro/nano-particle interaction can increase the roughness. The FESEM results indicated that increasing the pulse energy and number of pulses led to the formation of larger particle sizes and a more spherical and broad size distribution.

Table 3. EDX analysis of the prepared thin films.

Conditions	Cu	O	C	Na	Mg	Ca	Total
	Wt.%	Wt.%	Wt.%	Wt.%	Wt.%	Wt.%	Wt.%
700 mJ/600 pulses	26.19	38.22	14.6	12.06	4.36	4.81	100
700 mJ/1000 pulses	25.22	39.13	16.95	9.17	3.77	5.77	100
820 mJ/1000 pulses	30.28	34.79	14.35	11.05	4.7	4.82	100

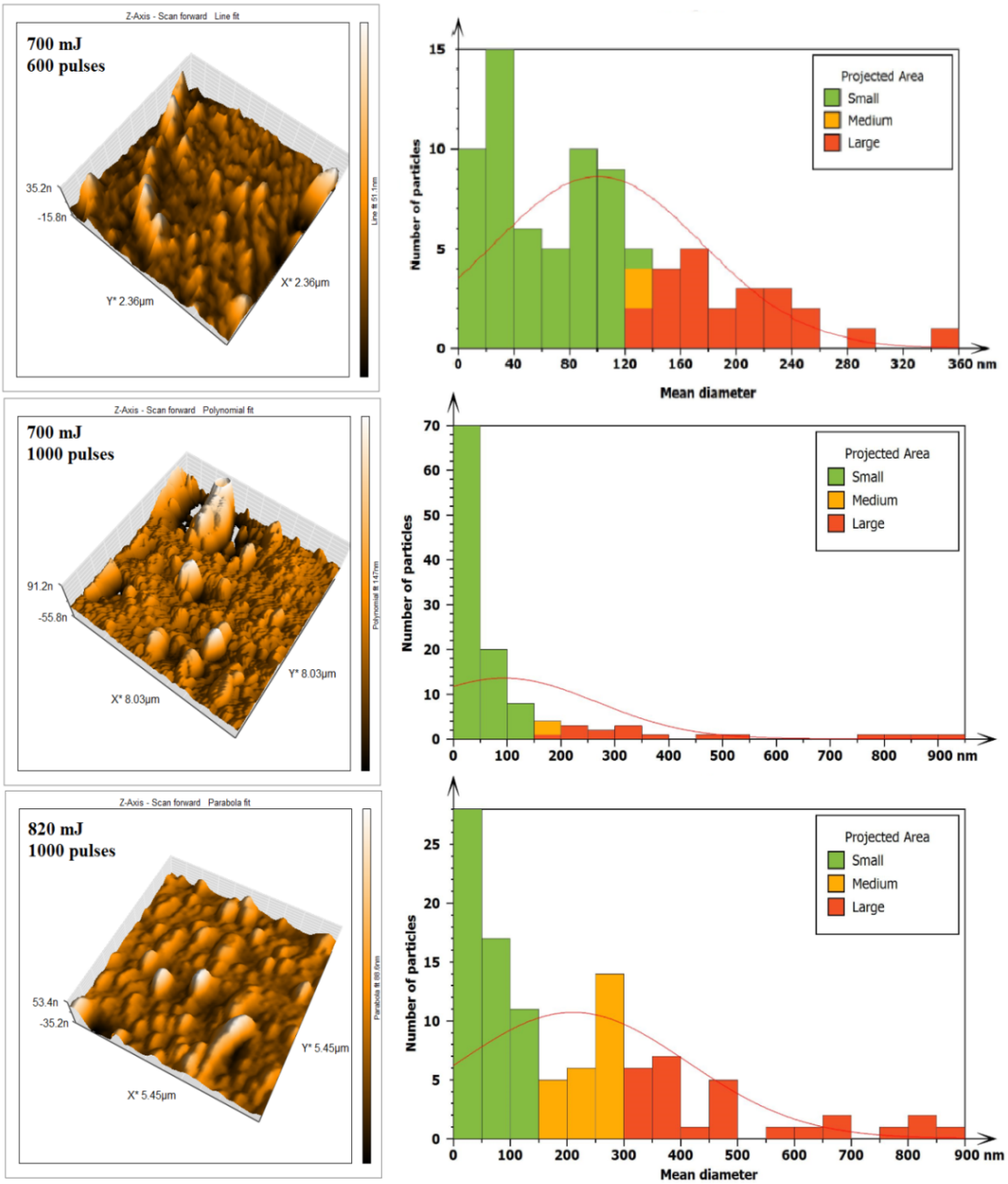

Figure 4. AFM 3D topography images of the CuO thin films at (a) 700 mJ/600 pulses, (b) 700 mJ/1000 pulses, and (c) 820 mJ/1000 pulses.

Table 4. AFM results for each condition.

Laser Energy (mJ)	Number of pulses	Average diameter	Roughness (nm)	RMS (nm)
700	600	100.8	26.58	5.7
700	1000	93.94	31.18	4.4
820	1000	210.6	20.89	3.2

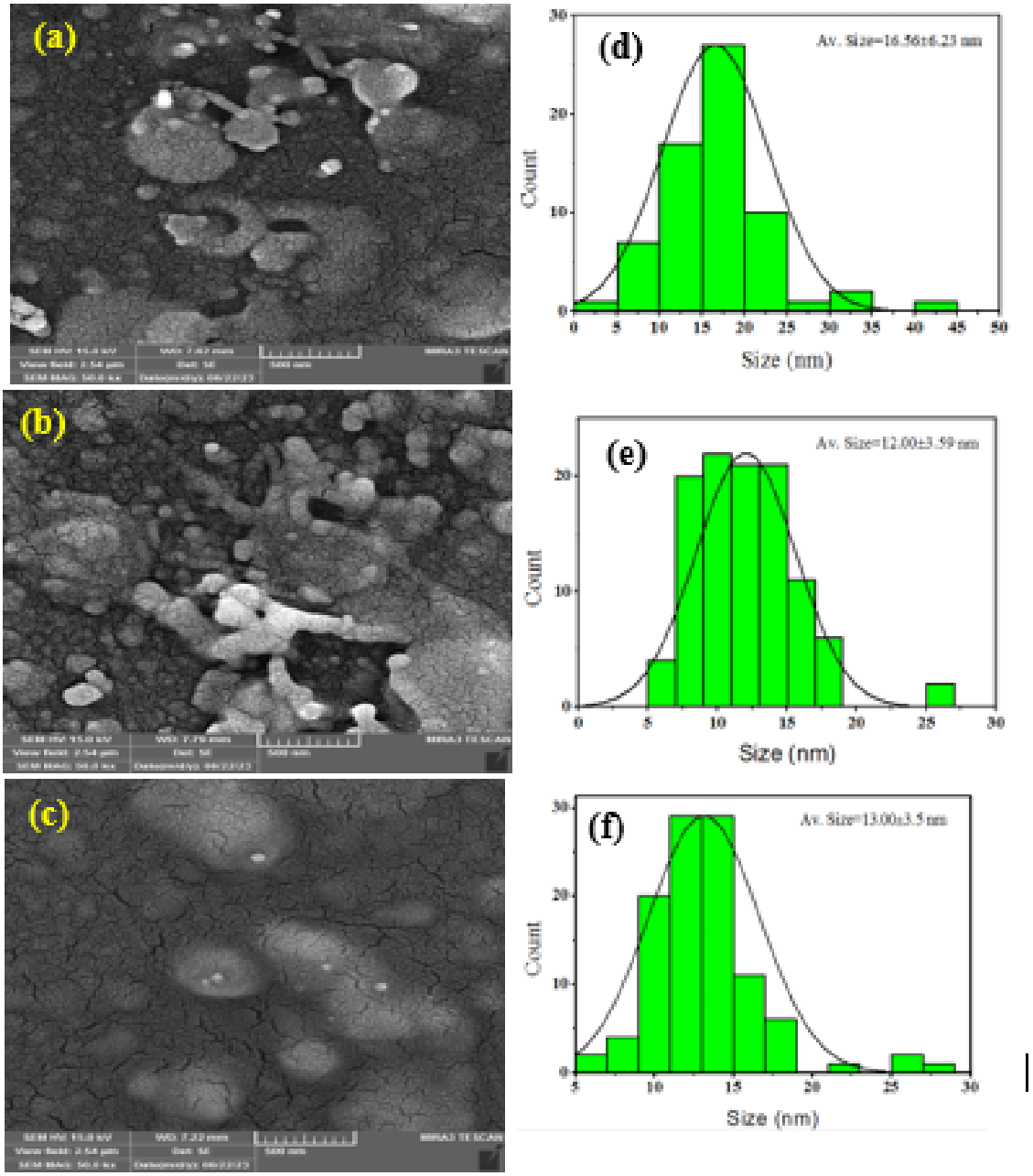

Figure 5. FESEM morphology images of the CuO thin films at (a) 700 mJ/600 pulses, (b) 700 mJ/1000 pulses, and (c) 820 mJ/1000 pulses, and (d-f) the CuO thin-film atom distribution histogram.

Acknowledgment

The authors thank the University of Anbar for granting access to laboratory facilities, which were important in completing this study.

Ethical approval
This manuscript does not report on or involve the use of any animal or human data or tissue. So the ethical approval is not applicable.

Authors Contributions
All the authors have participated sufficiently in the intellectual content, conception and design of this work or the analysis and interpretation of the data (when applicable), as well as the writing of the manuscript.

Availability of data and materials
The datasets generated and analyzed during the current study are available from the corresponding author upon reasonable request.

Conflict of Interests
The author declare that they have no known competing financial interests or personal relationships that could have appeared to influence the work reported in this paper.

References

[1] E. T. Efaz, M. M. Rhaman, S. Al Imam, K. L. Bashar, F. Kabir, M. E. Mourtaza, S. N. Sakib, and F. A. Mozahid. "A review of primary technologies of thin-film solar cells.". *Eng. Res. Express.*, **3**:032001, 2011. DOI: https://doi.org/10.1088/2631-8695/ac2353.

[2] Z. Yang, P.-F. Sun, X. Li, B. Gan, L. Wang, X. Song, H.-D. Park, and C. Y. Tang. "A critical review on thin-film nanocomposite membranes with interlayered structure: mechanisms, recent developments, and environmental applications.". *Environmental Science & Technology*, **54**:15563–583, 2020. DOI: https://doi.org/10.1021/acs.est.0c05377.

[3] H. T. Phan and A. J. Haes. "What does nanoparticle stability mean?". *J. Phys. Chem. C.*, **123**:16495–507, 2019. DOI: https://doi.org/10.1021/acs.jpcc.9b00913.

[4] V. S. Chandel, G. Wang, and M. Talha. "Advances in modelling and analysis of nano structures: a review.". *Nanotechnol. Rev.*, **9**:230–258, 2020. DOI: https://doi.org/10.1515/ntrev-2020-0020.

[5] I. Khan, K. Saeed, and I. Khan. "Nanoparticles: properties, applications and toxicities.". *Arab. J. Chem.*, **12**:908–931, 2019. DOI: https://doi.org/10.1016/j.arabjc.2017.05.011.

[6] J. M. Rzaij. "A novel room-temperature nitrogen dioxide gas sensor based on silver-doped cerium oxide thin film.". *Sensors Actuators A Phys.*, **363**:114748, 2023. DOI: https://doi.org/10.1016/j.sna.2023.114748.

[7] M. P. Nikolova and M. S. Chavali. "Metal oxide nanoparticles as biomedical materials.". *Biomimetics*, **5**:27, 2020. DOI: https://doi.org/10.3390/biomimetics5020027.

[8] S. K. Abdo and J. M. Rzaij. "Copper molarity effect on the optical properties of Cu2CdSnS4 quaternary thin films. ". *Iraqi J. Sci.*, **62**:1513–1523, 2021. DOI: https://doi.org/10.24996/ijs.2021.62.5.15.

[9] I. M. Ibrahim, J. M. Rzaij, and A. Ramizy. "Characterization OF CuPcTs/PS for NO_2 gas sensor. ". *Digest Journal of Nanomaterials and Biostructures*, **12**:1187–1196, 2017.

[10] A. A. Menazea, A. M. Mostafa, and E. A. Al-Ashkar. "Impact of CuO doping on the properties of CdO thin films on the catalytic degradation by using pulsed-Laser deposition technique.". *Opt. Mater. (Amst).*, **100**:109663, 2020. DOI: https://doi.org/10.1016/j.optmat.2020.109663.

[11] J. M. Rzaij and A. Mohsen Abass. "Review on: TiO_2 thin film as a metal oxide gas sensor. ". *J. Chem. Rev.*, **2**:114–121, 2020. DOI: https://doi.org/10.33945/SAMI/JCR.2020.2.4.

[12] O. S. Shawki and J. M. Rzaij. "Effect of Fe_2O_3 upper layer on structural, morphological, and photoluminescence characteristics of TiO_2 thin film prepared by chemical spray pyrolysis. ". *AIP Conf. Proc.*, **71**:020009, 2023. DOI: https://doi.org/10.1063/5.0112172.

[13] H. A. Tawfeeq and J. M. Rzaij. "Effect of Nb_2O_5 and PdO coatings on sensing characteristics of nanostructured CdO thin films.". *Iraqi Journal of Applied Physics*, **19**:3–12, 2023. DOI: https://doi.org/10.1016/j.fm.2007.12.005.

[14] H. A. Radwan, J. M. Marei, A. A. Khalefa, and J. M. Rzaij. "ZnO/PSi nanoparticles thin film for NO_2 sensing application prepared by pulsed laser deposition.". *Indian J. Phys.*, **98**:455–467, 2024. DOI: https://doi.org/10.1007/s12648-023-02806-9.

[15] A. A. Khalefa, H. A. Radwan, J. M. Marei, and J. M. Rzaij. "Effect of sintering temperature on the structural and morphological properties of hydroxyapatite prepared by precipitation method. ". *Key Eng. Mater.*, **944**:151–159, 2023.

[16] R. Panda, M. Patel, J. Thomas, and H. C. Joshi. "Pulsed laser deposited Cu_2O/CuO films as efficient photocatalyst.". *Thin Solid Films*, **744**:139080, 2022. DOI: https://doi.org/10.1016/j.tsf.2022.139080.

[17] A. A. Khalefa, J. M. Marei, H. A. Radwan, and J. M. Rzaij. "In_2O_3-CuO NANO-flakes prepared By spray pyrolysis for gas sensing application.". *Dig. J. Nanomater. Biostructures*, **16**:197–204, 2021. DOI: https://doi.org/10.15251/DJNB.2021.161.197.

[18] Z. Ibupoto, A. Tahira, H. Raza, G. Ali, A. Khand, N. Jilani, A. Mallah, C. Yu, and M. Willander. "Synthesis of heart/dumbbell-Like CuO functional nanostructures for the development of uric acid biosensor. ". *Materials (Basel)*, **11**:1378, 2018. DOI: https://doi.org/10.3390/ma11081378.

[19] B. Coşkuner Filiz. "The role of catalyst support on activity of copper oxide nanoparticles for reduction of 4-nitrophenol. ". *Adv. Powder Technol.*, **31**:3845–3859, 2020. DOI: https://doi.org/10.1016/j.apt.2020.07.026.

[20] J. M. Rzaij, A. S. Ibraheam, and A. M. Abass. "Cobalt effect on the growth of cadmium oxide nanostructure prepared by spray pyrolysis technique.". *Baghdad Sci. J.*, **18**:401–408, 2021. DOI: https://doi.org/10.21123/bsj.2021.18.2.0401.

[21] A. A. Nastulyavichus, S. I. Kudryashov, A. M. Emelyanenko, and L. B. Boinovich. "Laser generation of colloidal nanoparticles in liquids: key processes of laser dispersion and main characteristics of nanoparticles.". *Colloid J.*, **85**:233–250, 2023. DOI: https://doi.org/10.1134/S1061933X23600136.

[22] S. Ghosh, N. Dandapat, and V. K. Balla. "Preparation and in vitro characterization of fluroapatite based bioactive glass-ceramics for biomedical applications. ". *Mater. Today Proc.*, **2**:1326–1331, 2015. DOI: https://doi.org/10.1016/j.matpr.2015.07.050.

[23] Z. S. Hosseini, F. Haghparast, A. A. Masoudi, and A. Mortezaali. "Enhanced visible photocatalytic performance of un-doped TiO_2 nanoparticles thin films through modifying the substrate surface roughness.". *Mater. Chem. Phys.*, **279**:125530, 2022. DOI: https://doi.org/10.1016/j.matchemphys.2021.125530.

[24] J. M. Marei, A. A. Khalefa, Q. A. Abduljabbar, and J. M. Rzaij. "Nitrogen dioxide gas sensor of In_2O_3- ZnO polyhedron nanostructures prepared by spray pyrolysis. ". *J. Nano Res.*, **70**:41–51, 2021. DOI: https://doi.org/10.4028/www.scientific.net/JNanoR.70.41.

[25] N. F. Habubi J. M. Rzaij. "Enhancing the CO_2 sensor response of nickel oxide-doped tin dioxide thin films synthesized by SILAR method.". *J. Mater. Sci. Mater. Electron.*, **33**:11851–11863, 2022. DOI: https://doi.org/10.1007/s10854-022-08148-2.

[26] N. Mirghassemzadeh, M. Ghamkhari, and D. Dorranian. "Dependence of laser ablation produced gold nanoparticles characteristics on the fluence of laser pulse.". *Soft Nanosci. Lett.*, **03**:101–106, 2013. DOI: https://doi.org/10.4236/snl.2013.34018.

[27] S. I. Al-Nassar, F. I. Hussein, and A. K. M. "The effect of laser pulse energy on ZnO nanoparticles formation by liquid phase pulsed laser ablation.". *J. Mater. Res. Technol.*, **8**:4026–4031, 2019. DOI: https://doi.org/10.1016/j.jmrt.2019.07.012.